Impurity free intermixing InGaAs/GaAs strained multiple quantum well infrared photodetector

Alex S. W. Lee [1)], E. Herbert Li [1,2)], and Gamani Karunasiri [3)]

1. Dept. of Electrical and Electronic Engineering, University of Hong Kong, Pokfulam Road, Hong Kong
2. Division of Applied Sciences, Harvard University, Cambridge, MA 02138, USA
3. Department of Electrical Engineering, National University of Singapore, Singapore 119260

ABSTRACT

Interdiffusion effect has been investigated in highly strained InGaAs/GaAs multiple quantum well (MQW) infrared photodetector. Impurity -free interdiffusion techniques (IFVD) was utilized via rapid thermal annealing (RTA) using electron-beam evaporated SiO_2 cap layers at temperature 850 °C to study the optical and electrical properties of the interdiffused photodetector. Photoluminescence (PL) spectrum is blue shifted and PL linewidth remains almost the same, indicating no strain relaxation and deterioration of the heterostructure quality. Both transverse magnetic and transverse electric infrared intersubband transitions are retained and observed after intermixing. The absorption peak wavelength is red shifted continuously from the as grown 10.20 to the interdiffused 10.5 and 11.17 μm, respectively, without appreciable degradation in absorption strength for 5 and 10 s annealing. Annealed responsivity spectra of both 0° and 90° polarization are of compatible amplitude and red shifted but with narrower spectra linewidth. Dark current of the annealed devices is found to be an order of magnitude larger than the as-grown one at 77K.

Keywords: Multiple Quantum Well, Photodetector, Interdiffusion, Responsivity, Leakage current, Absorption

1. INTRODUCTION

Intersubband transitions (ITs) have attracted much research interest since the first experimental demonstration of large dipole moment in AlGaAs/GaAs multiple quantum wells (MQW).[1] Potential applications of IT in quantum wells have been investigated for infrared (IR) detectors,[2] and modulators.[3] High detectivities long wavelength infrared photodetectors (QWIPs) based on intersubband transitions cab be achieved and have been progressed rapidly in both bound-to-bound and bound-to-continuum[1] transitions.[4, 5] However, most of the studies have been limited to AlGaAs/GaAs multiple quantum wells (MQW) system owing to the mature growth and processing technology. However, due to the polarization selection rule, only incident light with a component of the electric field parallel to the growth direction (z axis) can be absorbed. Normal incidence is possible only with other optical coupling schemes. With the development of strained layer QW and bandgap engineering, high quality pseudomorphic QW is achievable. It has been demonstrated that normal incident strained InGaAs/GaAs[6] are possible without grating coupling. But the thermal stability of strained layers subjected to heat treatment is of prime importance and of great interest for optoelectronic device applications, especially for structure with higher In concentration. This is because highly strained heterostructure will result in smaller critical layer thickness and will increase the risk of strain relaxation by the generation of misfit dislocation. In this communication, we study the influence of dopant-enhanced layers interdiffusion on the performance of a highly strained n-doped $In_{0.3}Ga_{0.7}As/GaAs$ QWIP. We have observed not only the detection wavelength can be tuned continuously, but also the heterostructure quality is maintained. Both the transverse magnetic (TM) and transverse electric (TE) infrared (IR) intersubband transitions are observed after intermixing and the responsivity of these annealed devices is compatible with the as-grown one.

2. EXPERIMENT

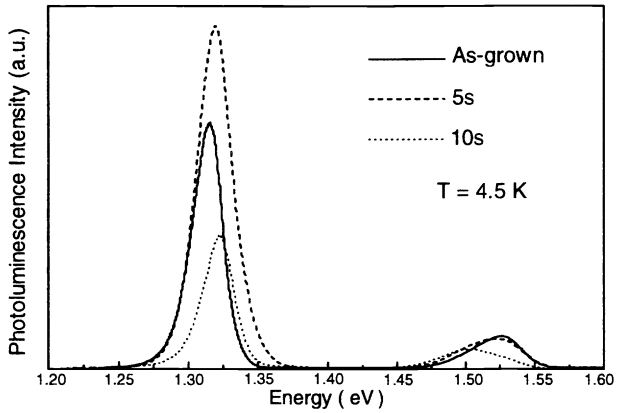

Fig. 1. Photoluminescence spectra of the as-grown, 5 s, and 10 s interdiffused InGaAs/GaAs MQW at T = 4.5 K.

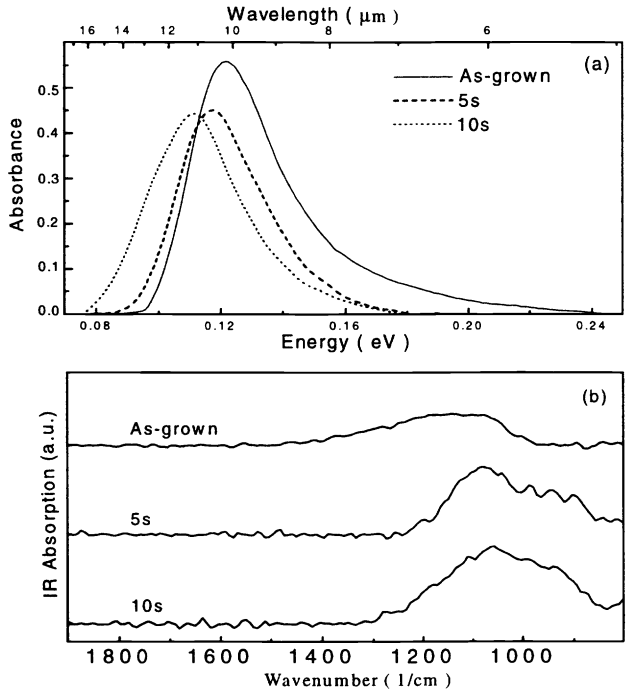

Fig. 2. Absorption spectra of the as-grown, 5 s, and 10 s annealed samples at 300 K as a function of wavelength for (a) 0° (TE + TM) polarization, and (b) 90° (TE) polarizations. (The curves have been shifted vertically for clarity.)

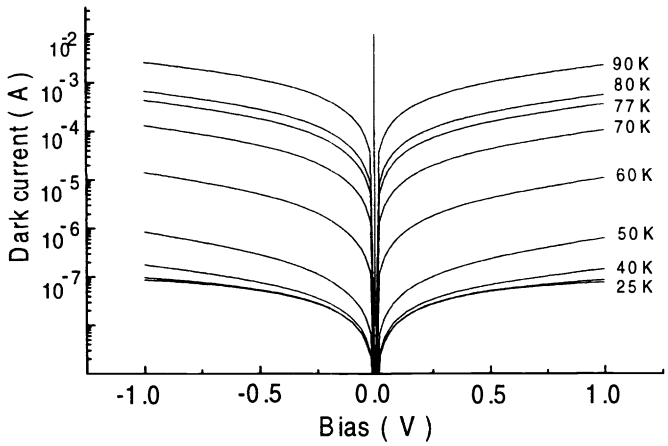

Fig. 3. I-V curve of the as-grown sample for 90 < T < 25 K as a function of bias.

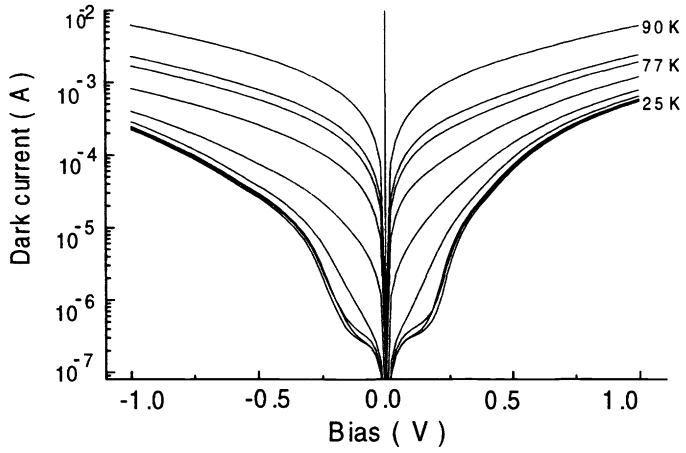

Fig. 4. I-V curve of the 5s annealed sample for 90 < T < 25 K as a function of bias.

The strained QWIP structure used in this study consists of 50 periods of 40 Å wide doped $In_{0.3}Ga_{0.7}As$ wells and 300 Å thick undoped GaAs barrier layers. The QW structure was sandwiched between a n^+ buffer (1 μm) and a cap layer (0.5 μm) for ohmic contacts. The wells were doped with Si at a density of about $2x10^{18}$ cm^{-3}. The structure was grown by molecular beam epitaxy (MBE) on a (100) semi-insulating GaAs substrate. Each QW was designed to have only one bound state inside the well and the first excited state in the continuum above the barrier. The energy difference between the first two eigenstates

corresponds to photon wavelength at 10 μm ($\hbar\omega$ = 124 meV) region. The structural quality of the as-grown superlattice was evaluated with by double-crystal x-ray diffraction (XRD). The angular separation of the satellite peaks shows one period QW thickness of 342 Å and the angular separation of the zero order peak from the substrate indicates In composition of 30.3%, very closed to the designed value. Intermixing was carried out using a halogen lamp annealing system (AST SHS10) with double strip graphite heater in nitrogen ambient. To facilitate interdiffusion, approximately 250 nm thick SiO_2 dielectric layer was deposited on the samples surface using electron-beam evaporator. One of the samples was annealed for 5s at 850 °C while the other for 10s at the same temperature. Photoluminescence (PL) measurements were performed at 4.5 K after annealing using the 514.5 nm Argon laser at a power of 200 mW. Fig. 1 shows the PL spectra of the as-grown and annealed MQW. It is observed that he PL peak shifts progressively to higher energy with increasing anneal time from as-grown 1.316 eV to 1.319 eV and 1.323 eV, respectively. The blue shift of the bandgap energy indicates the intermixing of group III elements near the heterostructure interfaces. The PL peak intensity of the 5s annealed sample is increased by nearly one fold while the 10s annealed sample also decreases by almost one fold relative to the as-grown sample. The full width at half maximum (FWHM) PL line-width does not vary very much as compare to the as-grown sample; less than 4 meV difference for the 5s annealed sample and 1 meV difference for the 10s annealed sample. The broadening for the 5 s annealed PL peak is believed to be due to the native defects near the surface incorporated during growth. Since the well width currently investigated is below the critical thickness for 30 % In concentration, the small variation in FWHM indicates that there is no strain relaxation or misfit dislocation formation during annealing and that there may even be a recovery of strain or an improvement in structural quality after RTA.[7, 8] Peaks were also observed at about 1.5 eV, which were red shifted with interdiffusion, in contrast to the PL peaks observed above. These peaks may due to the luminescence from GaAs either in the top cap layer or the bottom buffer layer.

3. RESULT AND DISCUSSION

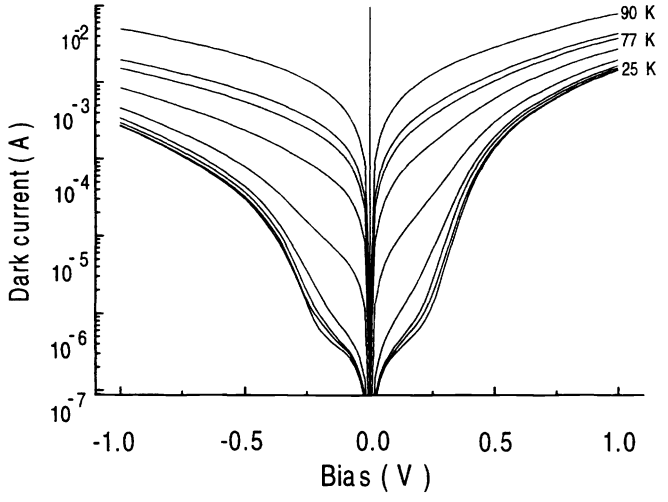

Fig. 5. I-V curve of the 10s annealed sample for 90 < T < 25 K as a function of bias.

Intersubband absorption measurement is taken using Nicolet Magna-IR 850 Fourier transform infrared spectrometer at room temperature with a 45° polished multipass waveguide geometry. Effect of interdiffusion on the optical properties of annealed QWs is evidenced in Fig. 2. Figure 2(a) shows the absorption spectra with 0° angle polarization, i.e., a mixture of TE and TM polarizations that contains a component of photon electric field along the growth (z) direction as well as a component in the plane of the layers. Whilst Fig. 2(b) shows the normal incident (TE) absorption spectra. As shown in the figures, the

absorption peaks are red shifted continuously for both angle polarizations. For 0° angle polarization, the absorption peaks of 5 and 10s annealed samples are shifted from as-grown 10.2 μm to 10.5 and 11.2 μm, respectively. While for TE polarization, the absorption peaks are shifted from 1124 cm^{-1} (8.9 μm) to 1080 (9.26 μm) and 1057 cm^{-1} (9.46 μm), respectively. The difference in the peak wavelength between the two polarizations mat arise due to the D_{2d} tetragonal perturbation of the local crystal and strain field effects on the QW.[9] The red shift of the absorption peaks indicates the bound state energy and the first excited state energy are being modified and/or the interdiffusion-induced changes in the doping-dependent depolarization shift,[10] which result in the postgrowth tuning of the absorption wavelength. Note for 0° polarization that the annealed absorption spectra reduced in amplitude and broadened proportionally with increasing annealed time. This can be attributed to the modification in the QW confinement profile and the redistribution of the dopant impurity. It is known that Ga is very soluble in SiO_2 at elevated temperature and therefore an increase in the concentration of group III vacancies is expected through the diffusion of Ga into the SiO_2 dielectric layer. This will in turn increase the dopant (Si) diffusion across the heterointerfaces into the undoped GaAs barrier and the cap layer, and subsequently converts it to a strongly n-typed material.[11]. The out diffusion of Si from the well reduces the free carrier concentration. Since absorption coefficient $\alpha(\hbar\omega) \propto \rho_s$, the two dimension electron density in the well, the reduction in the number of carriers available to be excited by the incident IR radiation may render to a reduction in the absorbance. In addition to the reduction in carrier density, the diffusion of dopant atoms across the heterointerfaces will enhance layers intermixing[11] and result in the modification of subband structure. Since the first excited energy remains in the continuum under different annealed conditions produced here, as can be seen from the characteristic features of bound-to-continuum intersubband transition in QWs[2] with high-energy tail and asymmetry of all the absorption spectra shown in Fig. 2(a), the interdiffused-induced changes in the subband structure may result in a smaller oscillator strength. Thus, the above two factors together with impurity scattering may give rise to the broadening and decreasing in amplitude of the absorption spectra.

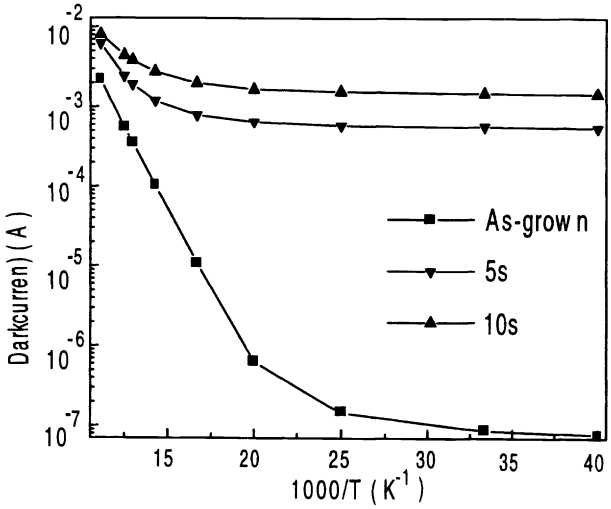

Fig. 6. Leakage current at v = 1 V as a function of the reciprocal of temperature in the range between 25-90 K.

Leakage current is measured at 77 K using 4156A Parameter Analyzer and cold finger. The (I-V) characteristic is shown in Fig. 3, 4, and 5 for the three devices. Note the asymmetry of the I-V curves between the two polarities. For the as-grown sample, leakage current is larger in reverse bias (i.e., mesa top negative) than in forward bias, which can be attributed to dopant migration to the growth front during growth.[2] While for the annealed devices the trend is just the opposite with leakage current larger at positive voltage. This is most probably due to the difference in diffusion rate of In and Ga species across the interfaces of the annealed QWs, which results in asymmetric barrier height[12] seen by the thermal excited electrons, or/and to the

re-distribution and segregation of the dopant impurity during RTA process as described in the previous section. In addition, the thinner 300 Å barrier and highly doped impurity concentration not only explain the asymmetry[13] I-V curves but also give rise to nearly an order of magnitude larger in leakage current than the as-grown one at 77 K. Figure 6 shows the leakage currents as a function of the reciprocal of temperature. It is interesting to note that the annealed leakage currents are not very sensitive to temperature variation from 25 to 90 K. The leakage currents remain approximately constant for T < 50 K and increase linearly with higher temperature. In this temperature range, the over all dark current increased nearly by one order of magnitude for the 5s annealed samples and by a factor of 8 for the 10s annealed sample, whereas the as-grown sample has increased by more than 5 orders of magnitude. Note also the leakage current of both the annealed devices is a few orders of magnitude larger than the as-grown one for T < 50 K. Since leakage current at low temperature is mainly tunneling in origin, the huge increase in leakage current is related to the defect assisted tunneling[14] as a result of the intermixing of Si and group III constituent atoms in the heterostructure,[11] which introduces defects (Ga vacancy) and dopant impurity into the barrier that results in significant electron tunneling through the defect states in the barrier. At temperature larger than this where thermionic emission mechanism is dominant, all leakage currents increase linearly to almost the same magnitude at T = 90K.

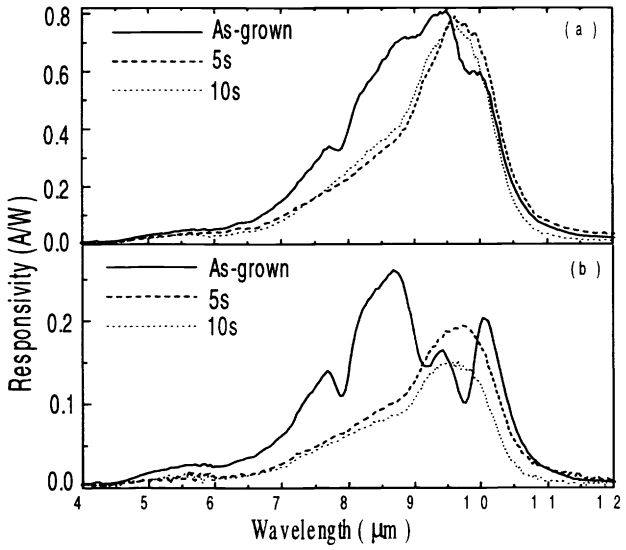

Fig. 7. Photoresponse spectra at 25 K of the as-grown, 5 s, and 10 s annealed samples bias at 2.5 V, 1.05 V, and 1.65 V for (a) 0° polarization, and (b) 90° polarization, as a function of wavelength.

Mesa diodes (200 x 200 μm) were fabricated by standard lithographic technique and 45° facet was polished at one end of the sample for responsivity measurement. The photocurrent was measured using grating monochromator and glowbar source with lock-in detection. Polarizer was inserted before the glowbar source in order to study the polarization dependence of the photoresponse. Figure 7 show the response spectra for 0° and 90° polarizations, respectively, as a function of wavelength at 25 K. For both polarization responsivity spectra, the peak positions were observed to be red shifted and independent of polarization. Note the as-grown spectra in both figures that other than the designed peak, there are a few satellite peaks appear in the spectral at rather identical wavelength positions for both polarizations. Since the QW structure is designed only to have the first excited state above the barrier, these satellite peaks are most probably due to the intersubband transition from the bound state E_1 to other excited states in the continuum[15] or to the interaction between the first excited state E_2 and other states in the continuum.[16] With the modification of QW structure by means of interdiffusion, the annealed spectra in Fig. 4 show that regardless of polarization, all these peaks are subdued except the designed main transition peak. For 0° polarization, the

corresponding responsivity amplitudes 0.8, 0.79, and 0.77 A/W do not vary much for the as-grown and annealed detectors, as shown in Fig. 7(a), where all the spectra have almost identical rising edge. This is as expected since the MQW properties and its structure have not been substantially modified or deteriorated after interdiffusion, once the photoexcited carriers overcome the threshold barrier into the continuum states they are ready to be collected as photocurrent. The normal incident absorption, which is believed to be the result of band-mixing effects induced by the coupling between the conduction and valence[17] and is usually forbidden in conventional polarization selection rule,[1] is preserved after interdiffusion. It is also interesting to note in Fig. 7(b) that for 90° polarization, the significant peak responsivity of the as-grown spectrum does not occur at the designed wavelength. However, this is not the case for the annealed spectra where the dominant state equals to the designed transition peak and red shifts with interdiffusion. The bias dependent responsivities for both polarities are shown in Fig. 8. The effect of interdiffusion on the transport properties of MQW is evidence in the figure. Notice that the as-grown responsivity at reverse bias (R = 1 A/W) is larger than at forward bias (R = 0.8 A/W). This is consistent with the I-V characteristic under opposite bias polarity as a result of dopant diffusion into the barrier during growth that creates an asymmetric energy band bending in the barriers and a thinner effective barrier thickness. It is just the opposite for the interdiffused responsivity since the leakage current is larger under forward bias due to the random distribution of the dopant and alloy species. Both the forward bias annealed responsivities are a few factors larger than under reverse bias. Note also that the bias dependent annealed responsivity saturated and decreased in amplitude at bias lower than the as-grown one. This is most probably due to the intervalley scattering where the electrons in the Γ valley scatter into the L or the X valley minima under an applied electric field as a result of interdiffusion. . Since intermixing can modify the subband structure and the first excited state is in the continuum, it is possible that other valleys can be brought close to or under the first excited state via intermixing such that electrons scatter into these valleys, losing its momentum and reducing in responsivity.

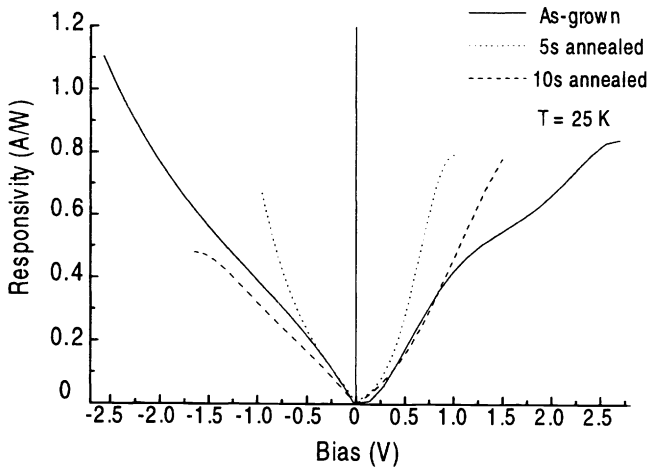

Fig. 8 Bias dependent responsivity of as-grown (solid line), 5s annealed (dot line), and 10s annealed (dash line) samples as a function of bias.

4. CONCLUSION

In conclusion, high In composition pseudomorphic interdiffused InGaAs/GaAs QWIP using dopant-enhanced vacancy interdiffusion has been demonstrated for its post-growth tunability. No strain relaxation and deterioration in the MQW structure are observed. The TE polarization infrared intersubband transition, as a result of the band-mixing effects, is preserved. Both 0° and 90° polarizations absorption peaks are red shifted with respect to the as-grown one without much degradation in absorption strength. Photoresponse peaks due to resonances in the continuum states are subdued after interdiffusion. The annealed photoresponse spectra for 0° polarization are comparable to the as-grown device with a narrower FWHM, while the designed

photoresponse peak becomes dominant at 90° polarization. Dark current of the annealed devices is about an order higher in amplitude than the as-grown one at 77 K. The I-V characteristic is less sensitive to the variation in temperature from 25-90 K where the overall dark current of both the annealed devices are varied in between a range of about one order in magnitude.

5. ACKNOLEDGEMENT

This work is support in part by the HKU-CRCG, RGC-Earmarked Research Grants and Academic Research Fund of National University of Singapore. The author would like to thank Prof. S. J. Chua for valuable suggestions, T. Mei, and Dr. S. J. Xu for technical assistance.

6. REFERENCE

1. L. C. West and S. J. English, "First observation of an extremely large-dipole infrared transition within the conduction band of a GaAs quantum well," Appl. Phys. Lett. **46**, 1156 (1985).
2. B. F. Levine, A. Zussman, S. D. Gunapala, M. T. Asom, J. M. Kuo, and W. S. Hobson, "Photoexcited escape probability, optical gain, and noise in quantum well infrared photodetectors," J. Appl. Phys. Lett. **72**, 4429 (1992).
3. A. Tomita, Y. Kohga, and A. Suzuki, :5:1 OnOff Contract InGaAs/InP Multiple Quantum Well Fabry-Perot Etalon Modulator", Appl. Phys. Lett. **55**, pp1817-1819 (1989).
4. B. F. Levine, A. Zussman, S. D. Gunapala, M. T. Asom, J. M. Kuo, and W. S. Hobson, "Photoexcited escape probability, optical gain, and noise in quantum well infrared photodetectors," J. Appl. Phys. Lett. **72**, pp. 4429-4442, (1992)
5. B. F. Levine, C. G. Bethea, G. Hasnain, V. O. Shen, E. Pelve, R. R. Abbott, and S. J. Hsieh, "High sensitivity low dark current 10 μm GaAs quantum well infrared photodetectors", Appl. Phys. Lett. **56**, 851 (1990).
6. R. P. G. Karunasiri, J. S. Park, J. Chen, and R. Shih, "Normal incident InGaAs/GaAs Multiple quantum well infrared detector using electron intersubband transitions," Appl. Phys. Lett. **67**, pp. 2600-2602, (1995).
7. Elman, E. S. Koteles, P. Melman, C. Jagannath, C. A. Armiento, and M. Rothman, "Effect of heat treatment on InGaAs/GaAs quantum wells," J. Appl. Phys. **68**, pp. 1351-1353, (1990).
8. S. Bürker, M. Baeumler, J. Wanger, E. C. Larkins, W. Rothemund, and J. D. Ralston, "Influence of interdiffusion processes on optical and structural properties of pseudomorphic $In_{0.35}Ga_{0.65}As$/GaAs multiple quantum well structures," J. Appl. Phys.h. **79**, pp. 6818-6824, (1996).
9. L. H. Peng, J. H. Smet, T. P. E. Broekaert, and C. G. Fon stad, "Transverse electric and transverse magnetic polarization active intersubband transitions in narrow InGaAs quantum will," Appl. Phys. Lett. **61**, pp. 2078-2080, (1992).
10. J. D. Ralston, M. Ramsteiner, B. Discher, M. Maier, G. Brandt, P. Koidl, and D. J. As, "Intersubband transitions in partially interdiffused GaAs/AlGaAs multiple quantum-well structrue," J. Appl. Phys. **70**, pp. 2195-2199, (1991).
11. D. G. Deppe and N. Holonyak, Jr., "Atom diffusion and impurity-induced layer disordering in quantum well III-V semiconductor heterostructures", J. Appl. Phys. **64**, R93 (1988).
12. S. W. Lee and E. H. Li, "Effects of interdiffusion of quantum well infrared photodetector," Appl. Phys. Lett. **69**, pp. 3581-3583, (1996).
13. H. C. Liu, Z. R. Wasilewski, M. Buchanan, and Hanyou Chu, "Tunneling emitter undoped quantum-well infrared photodetector.", Appl. Phys. Lett. **63**, pp. 761-763, (1993).
14. G. M. William, R. E. DeWames, C. W. Farley, and R. J. Anderson, "Excess tunnel currents in AlGaAs/GaAs multiple quantum well infrared detectors.", Appl. Phys. Lett. **60**, pp. 1324 (1992).
15. K. M. S. V. Bandara, B. F. Levine, and M. T. Asom, "Segregation of Si doping in GaAs-AIGaAs quantum wells and the cause of the asymmetry in the current-voltage characteristics of intersubband infrared detectors." J. Appl. Phys. **74**, pp. 346-350, (1993).
16. K. K Choi, M. Taysing-Lara, P. G. Newman, and W. Chang, "Wavelength tuning and absorption line shape of quantum well infrared photodetectors." Appl. Phys. Lett. **61**, pp. 1781-1783, (1992).
17. L. H. Peng and C. G. Fonstad, "Multiple coupling effects on electron quantum well-intersubband transitions," J. Appl. Phys. **77**, pp. 747-754, (1995).